Available online at www.sciencedirect.com
SCIENCE DIRECT®
International Journal of Heat and Mass Transfer 48 (2005) 4333–4341
International Journal of HEAT and MASS TRANSFER
www.elsevier.com/locate/ijhmt

Development of a heat transfer dimensionless correlation for spheres immersed in a wide range of Prandtl number fluids

Blas Melissari, Stavros A. Argyropoulos *

Department of Materials Science and Engineering, University of Toronto, 184 College Street, Toronto, ON, Canada M5S 3E4

Received 15 September 2004; received in revised form 27 May 2005
Available online 19 July 2005

Abstract

In this paper a computational approach is employed to derive a dimensionless heat transfer correlation for forced convection over a sphere. This correlation is applicable to fluids with a wide range of Prandtl numbers. The lower end of this range includes the Prandtl number for liquid sodium ($Pr \approx 0.003$), whereas the upper end includes the Prandtl number for water ($Pr \approx 10$).

$$Nu = 2 + 0.47Re^{1/2}Pr^{0.36} \quad 3 \times 10^{-3} \leqslant Pr \leqslant 10^{1}; \quad 10^{2} \leqslant Re \leqslant 5 \times 10^{4}$$

The model predictions derived from this research were validated extensively. First, the model was tested in two liquid metals, and subsequently it was compared with existing experimental data involving water. Both verification procedures have shown very good agreement between experimental results and model predictions. Multiple regression was employed to derive the above mentioned correlation. A detailed description of various steps used is described here.

Keywords: Liquid metals; Heat transfer coefficient; Modeling; Experimental; Forced convection; Nusselt number

1. Introduction

There is a derth of dimensionless convective heat transfer correlations applicable to fluids such as liquid metals. Knowledge of heat transfer rates from particles at high flux levels has become increasingly important to the design of energy transfer systems and metallurgical processes in general.

Theoretical as well as experimental approaches have been carried out to analyze the heat transfer in liquid metals. Hsu [1] and Sideman [2] have derived equations for heat transfer from a sphere to a liquid metal by assuming a potential flow around the sphere. Kreith et al. [3] performed an experimental investigation of rotating metallic spheres in liquid mercury and suggested a correlation for forced convection. Witte [4] performed experiments on heat transfer from a non-melting sphere to liquid sodium and obtained an equation relating the Nusselt number to Reynolds and Prandtl numbers. Argyropoulos and Mikrovas [5,6] immersed spheres in liquid aluminum and steel and found correlations for forced and natural convection based on the measurement of the melting times of the spheres. Many

* Corresponding author. Tel.: +1 416 978 5302; fax: +1 416 978 4155.
E-mail address: stavros.argyropoulos@utoronto.ca (S.A. Argyropoulos).

0017-9310/$ - see front matter © 2005 Elsevier Ltd. All rights reserved.
doi:10.1016/j.ijheatmasstransfer.2005.05.025

Nomenclature

A	area, m^2
CV	control volume
D	diameter, m
g	gravity, m/s^2
Gr	Grashof number, $g\beta\rho^2\mathrm{SPH}D^3/\mu^2$
h	heat transfer coefficient, W/(m^2 °C)
k	thermal conductivity, W/(m °C)
c	specific heat capacity (J kg^{-1} °C^{-1})
LH	latent heat, J/kg
m	mass, kg
MT	melting time, s
Nu	Nusselt number, hD/k
Pr	Prandtl number, $\mu c/k$
Re	Reynolds number, $\rho uD/\mu$
SPH	superheat, $(T_\infty - T_\mathrm{m})$ in °C
T	temperature, °C
t	time, s
Δt	time step, s
u	velocity, m/s
V	volume, m^3

Greek symbols

β	thermal expansion coefficient, 1/°C
μ	dynamic viscosity, kg/ms
ρ	density, kg/m^3

Subscripts

0	initial condition
∞	liquid condition far from sphere
F	factor
m	melting point (liquidus)
max	maximum
S	solid condition (solidus)
FC	forced convection
corr	correlation
model	modeling prediction
exper	experimental result

investigators studied the heat transfer characteristics of solid spheres to fluids with Prandtl number around unity ($Pr_{\mathrm{air}} \approx 0.7$; $Pr_{\mathrm{water}} \approx 10$). McAdams [7] compiled numerous experimental results and correlated all of them into a single empirical correlation valid for air and water. Yuge performed pioneering experimental work on the heat transfer from a sphere to air under mixed convection [8], suggesting procedures for predicting the Nusselt number. Vliet and Leppert [9] developed correlations for spheres in water. Hieber et al. [10] studied the spherical system analytically, but their study was limited to small Reynolds numbers.

Some researchers studied the melting dynamics of ice spheres in water at different convective regimes. Vanier and Tien [11] performed experiments on the melting of a submerged ice sphere in water, calculating the melting rate by weighing the sphere. Solomon [12] obtained a solution for the melting of a sphere in convection as a function of the average diameter and heat flux. Eskandari et al. [13] reported on a series of experiments to study the forced convection heat transfer from a flowing stream of water to an ice sphere. Anselmo et al. [14,15] undertook an extensive theoretical and numerical analysis of melting both full and partially submerged ice spheres in a pool of water. Aziz et al. [16] and Hao et al. [17] performed measurements of the heat transfer coefficient in the water system by measuring the melting time of ice spheres in forced convection. Mukherjee et al. [18], McLeod et al. [19] and Hao et al. [20] conducted visualization studies of ice spheres melting in water under a mixed convection regime.

In terms of mixed convection around a sphere in liquid metals, the work of Kreith and his associates is particularly noteworthy [21,3]. By performing experimental measurements of rotating spheres in media as diverse as air and mercury, they concluded that if the buoyancy parameter (Gr/Re^2) is less than 0.3, then natural convection is negligible, i.e., its effect is lower than 5% as far as the heat transfer is concerned. This value agrees with the theoretical derivation by Sparrow et al. [22]. Numerical model predictions regarding the influence of natural convection on the total melting time of spheres has been published by Melissari and Argyropoulos [23]. They concluded that for values of the buoyancy parameter lower than the range $Gr/Re^2 = 0.5$–1.0, the total melting time is not affected by natural convection effects. Table 1 summarizes all known correlations for heat transfer around spheres and their range of applicability. As seen from this summary, all the correlations correspond to either a single or to a narrow range of Prandtl numbers.

In this paper a numerical model is developed. This model allows predictions to be made of melting times of various spheres immersed in fluids with different Prandtl numbers. An extensive and diverse model verification took place. The first two sets of experimental work for this verification involved liquid metals such as aluminum ($Pr_{\mathrm{Al}} = 0.015$) and a magnesium alloy AZ91 ($Pr_{\mathrm{AZ91}} = 0.024$). In the third set, the model was verified with another set of experimental work reported in literature involving water ($Pr_{\mathrm{water}} \approx 10$). With the verified numerical model, predictions of sphere melting times

Table 1
Nusselt number for forced convection around spheres

Authors	Applicability	Nusselt number correlated
Hsu [1]	$Pr < 1$; $Re \leqslant 2\times10^5$	$0.921(Re\cdot Pr)^{1/2}$
Sideman [2]	$Pr < 1$; $Re \leqslant 2\times10^5$	$1.13(Re\cdot Pr)^{1/2}$
Kreith [3]	$Pr = 10^{-2}$; $7\times10^4 \leqslant Re \leqslant 10^6$	$0.178Re^{0.375}$
Witte [4]	$Pr = 10^{-3}$; $3\times10^4 \leqslant Re \leqslant 2\times10^5$	$2+0.386(Re\cdot Pr)^{1/2}$
Argyropoulos [5]	$10^{-2} \leqslant Pr \leqslant 10^{-1}$; $Re \leqslant 3\times10^4$	$2+1.114Re^{0.557}Pr^{0.914}$
Whitaker [28]	$Pr = 0.7$; $Re \leqslant 8\times10^4$	$2+[0.4Re^{1/2}0.06Re^{0.67}]Pr^{0.4}$
Vliet and Leppert [9]	$Pr \sim 10$; $Re \leqslant 10^5$	$(2.7+0.12Re^{0.66})Pr^{1/2}$
Aziz et al. [16]	$Pr \sim 10$; $3\times10^3 \leqslant Re \leqslant 3\times10^4$	$0.991Re^{0.527}Pr^{0.043}$
Hao et al. [17]	$Pr \sim 10$; $Re \leqslant 3\times10^3$	$1.015Re^{0.48}Pr^{0.23}$
McAdams [7]	$Pr \geqslant 0.7$; $Re \leqslant 2\times10^5$	$2+0.6Re^{1/2}Pr^{1/3}$

were carried out for fluids with very wide range of Prandtl numbers. The lower end of this range includes the Prandtl number for liquid sodium ($Pr \approx 0.003$), whereas the upper end includes the Prandtl number for water ($Pr \approx 10$). Melting times, derived from the model predictions, were utilized. From these model predictions, a dimensionless correlation derived using multiple regression analysis. In this case the Nusselt number is expressed as a function of the Reynolds and Prandtl numbers.

2. Mathematical considerations

2.1. Calculating the Nusselt number from the melting time

By applying a heat balance to the sphere, it is possible to relate the total melting time to the Nusselt number. It is assumed that the sphere is subject to uniform melting, meaning that we will calculate the Nusselt number averaged over the entire surface as opposed to the localized coefficient. The instantaneous heat balance is shown in Eq. (1).

$$h * A * \mathrm{SPH} * \mathrm{d}t = \rho * \mathrm{LH} * \mathrm{d}V \tag{1}$$

where $h = \dfrac{Nu * k_\infty}{D}$.

In this context, D represents the diameter as a variable and D_0 is the initial diameter of the sphere. The sensible portion of the heat supplied to the sphere is not included because it is assumed that the shell is formed at the expense of heating the sphere up to its melting point. The volume, surface area and volume differential of a sphere are as follows:

$$\begin{aligned} V &= \frac{1}{6}\pi * D^3 \\ A &= \pi * D^2 \\ &\Rightarrow \mathrm{d}V = \frac{1}{2}\pi * D^2\mathrm{d}D = \frac{1}{2}A\mathrm{d}D \end{aligned} \tag{2}$$

The Nusselt number can be expressed in terms of the diameter as $Nu = C_1Re^{1/2} = C_2D^{1/2}$ for forced convection. At this stage it would be desirable to express the exponent in a parametric way since it would be valuable to find the parameter from the equation rather than setting it at a certain fixed value. Hence this relationship becomes: $Nu = C_1Re^{n_{\mathrm{FC}}} = C_2D^{n_{\mathrm{FC}}}$. Substituting Nu and $\mathrm{d}V$ in the differential heat balance (1), and by rearrangement we obtain:

$$\begin{aligned} & h * \mathrm{SPH} * \mathrm{d}t = \frac{1}{2}\rho * \mathrm{LH} * \mathrm{d}D \\ & \Rightarrow C_2 * k_\infty * \mathrm{SPH} * \mathrm{d}t = \frac{1}{2}\rho * \mathrm{LH} * D^{(1-n_{\mathrm{FC}})} * \mathrm{d}D \end{aligned} \tag{3}$$

The LHS of the equation can be integrated in time, whereas the RHS of the equation has to be integrated between the initial diameter (D_0) and the maximum diameter reached by the sphere when the shell is formed ($D_{\max}$), and then from $D_{\max}$ to $D = 0$. This yields the following:

$$\begin{aligned} & C_2 * K_\infty * \mathrm{SPH} * \int_0^{\mathrm{MT}} \mathrm{d}t \\ & = \frac{1}{2}\rho * \mathrm{LH}\left(\int_{D_0}^{D_{\max}} D^{(1-n_{\mathrm{FC}})}\,\mathrm{d}D + \int_{D_{\max}}^{0} D^{(1-n_{\mathrm{FC}})}\,\mathrm{d}D\right) \\ & \Rightarrow C_2 * k_\infty * \mathrm{SPH} * \mathrm{MT} \\ & = \frac{1}{2}\rho * \mathrm{LH} * \frac{(2D_{\max}^{(2-n_{\mathrm{FC}})} - D_0^{(2-n_{\mathrm{FC}})})}{2-n_{\mathrm{FC}}} \end{aligned}$$

Substituting $Nu = C_2D^{n_{\mathrm{FC}}}$ and rearranging terms, we obtain a relationship between the melting time and the Nusselt number as a function of the initial diameter D_0 as seen in Eq. (4).

$$Nu = \left(2\left(\frac{D\max}{D_0}\right)^{(2-n_{\mathrm{FC}})} - 1\right)\frac{\rho * \mathrm{LH} * D_0^2}{2*(2-n_{\mathrm{FC}})*k_\infty * \mathrm{SPH} * \mathrm{MT}} \tag{4}$$

Assuming that the diameter can be obtained from the mass of the sphere using a relationship of the form $m \propto D^3$; we can express the Nusselt number as Eq. (4).

$$Nu = \mathrm{MT_F} * \frac{\rho * \mathrm{LH} * D_0^2}{2*(2-n_{\mathrm{FC}})*k_\infty * \mathrm{SPH} * \mathrm{MT}} \tag{5}$$

where $\mathrm{MT_F} = 2m_{\mathrm{F}}^{1/3(2-n_{\mathrm{FC}})} - 1$; with $m_{\mathrm{F}} = \frac{m_{\max}}{m_0}$.

The melting time factor, MT_F, affects the total time of the immersed sphere and is caused by the shell formation upon immersion. It is calculated based on the mass increase of the sphere. The mass factor, m_F, is calculated as the ratio between the maximum mass of the sphere (m_{max}) and the initial mass (m_0). In the subsequent sections these factors will be estimated. For a value of $n_{FC} = \frac{1}{2}$, the Nusselt number for forced convection is Eq. (6).

$$Nu = MT_F \frac{\rho * LH * D_0^2}{3 * k_\infty * SPH * MT} \tag{6}$$

where

$$MT_F = 2m_F^{1/2} - 1 \tag{7}$$

2.2. Mathematical modeling of the melting sphere

The problem of a melting sphere is modeled as a three-dimensional system in Cartesian coordinates of fluid flow and heat transfer coupled by the presence of natural convection. A detailed explanation, including the equations solved and numerical scheme implemented, can be found in [24]. A schematic of the domain used for the calculations can be seen in Fig. 1. The thermophysical properties of aluminum and AZ91 used in the model are summarized in Table 2.

2.3. Results of the numerical model

The total melting times of 3 cm and 7 cm aluminum spheres as a function of the bath velocity are shown in Figs. 2 and 3, respectively. For $u = 0$ cm/s, the solution represents the pure natural convection solution. Plots showing velocity vector and isotherms can be found in [24].

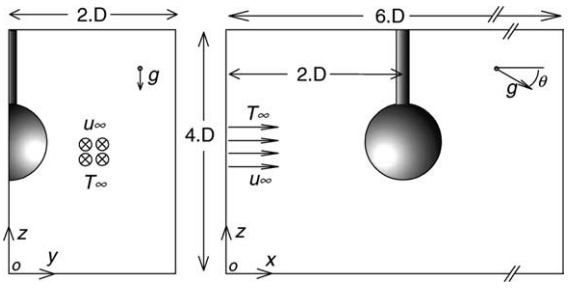

Fig. 1. Domain used for the numerical simulations.

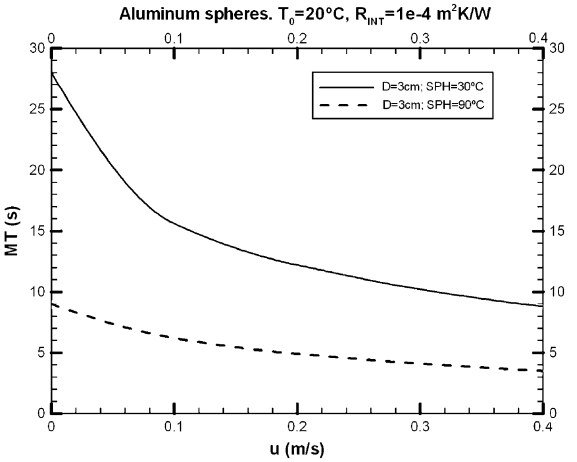

Fig. 2. Melting times of 3 cm aluminum spheres.

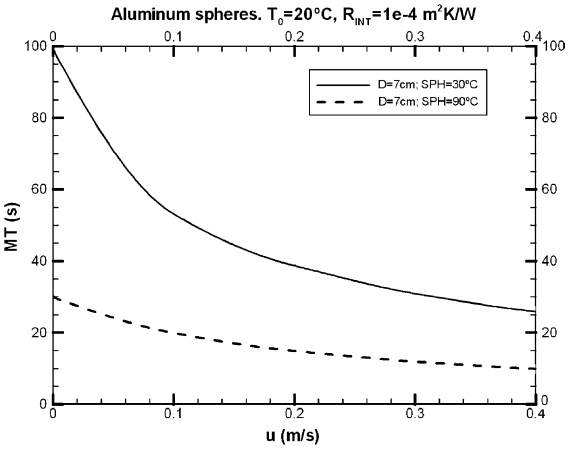

Fig. 3. Melting times of 7 cm aluminum spheres.

2.3.1. Melting time factor

By running the model for different sphere initial temperatures, T_0, the melting time factor was estimated. This was carried out by calculating the ratio between the melting time at a given initial temperature, T_0, and an initial temperature, T_m. Fig. 4 shows the melting time factor, MT_F, for aluminum spheres under different

Table 2
Thermophysical properties of materials used, SI units [29]

Material	k_S	k_∞	c_S	c_ρ	ρ	μ	β	T_S	T_M	LH
Al	220	90	1100	1000	2400	1.2×10^{-3}	1.3×10^{-4}	660	660	3.95×10^{5}
AZ91	60	80	1200	1400	1750	1.4×10^{-3}	1.2×10^{-4}	437	600	3.7×10^{5}
Water	2.2	0.6	2100	4200	1000	1.2×10^{-3}	4.0×10^{-4}	0	0	3.4×10^{5}

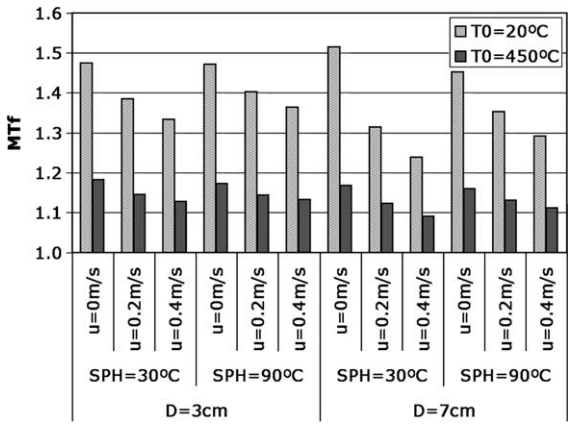

Fig. 4. Melting time factor for different operating parameters in the aluminum system (numerical model).

conditions of diameter, superheat and velocity, for $T_0 = 20\ ^\circ\mathrm{C}$ and $T_0 = 450\ ^\circ\mathrm{C}$. The values of $\mathrm{MT_F}$ do not vary significantly with the diameter and superheat, but change from $\mathrm{MT_F} = 1.5$ in natural convection to $\mathrm{MT_F} = 1.3$ for $u = 0.4$ m/s, mainly due to the fact that the melting is non-uniform for the higher values of velocity in forced flow. If the initial temperature is closer to the melting point of the material, the shell increase is much lower and subsequently the melting time factor would be very close to unity. In any case, there is no more than a 20% increase in the melting time for $T_0 = 450\ ^\circ\mathrm{C}$; with little variation in diameter, superheat, or even velocity.

The maximum mass increase observed in the numerical simulations was of the order of 50%; meaning we obtain a mass factor $m_\mathrm{F} = 1.5$. Using the expression for the melting time factor, $\mathrm{MT_F} = 2m_\mathrm{F}^{1/2} - 1$, we observe that if we use the measured values of mass increase, we obtain a value that is in agreement with the results of the numerical simulation: $\mathrm{MT_F} = 2(1.5)^{1/2} - 1 = 1.45$

Some specific measurements were carried out where the spheres were extracted prior to complete melting. In this way, the shell formed around the sphere could be measured and the melting time factor could be estimated. The maximum mass increase observed experimentally was of the order of 40–60%.

It is convenient to minimize the error involved in the estimation of these factors. A possible way is to perform experiments with heated spheres thus reducing the mass increase, as observed numerically in Fig. 4. Ideally, a solid sphere at its melting point will not form a shell. However, it is highly impractical to immerse such spheres mainly due to their poor mechanical integrity. Nevertheless, some experiments were carried out with Aluminum spheres preheated at $T_0 = 450\ ^\circ\mathrm{C}$ simply to determine its experimental feasibility. These were performed using 3 cm and 5 cm spheres in 60 °C superheat bath in the velocity range 0–0.3 m/s.

3. Validation of the numerical model

In order to validate the numerical model developed, a series of tests were carried out to run under the characteristics of a set of established solutions found in the literature, both analytical and experimental.

3.1. Paterson point heat source analytical solution

First, a one dimensional heat diffusion/melting system was developed in spherical coordinates to solve for Paterson's point heat source analytical solution [25]. The conditions chosen emulate the very high heat transfer rates found in liquid metals. This tests the Heat Integration Algorithm as well as the ability of the code to handle a large heat transfer rate under a hypothetical heat source. A more detailed explanation about this validation can be found in [26].

3.2. Experimental results in melting gallium

Second, a two-dimensional convective/melting system in rectangular coordinates was developed in order to compare it with the experimental study of the melting of gallium in an enclosure by Gau and Viskanta [27]. This tests the Heat Integration Algorithm as well as the natural convection induced flow in a liquid metal (complete validation results can be found in [26]).

3.3. Experimental results in melting ice

Third, the three-dimensional model developed for liquid metals was set to run using the thermophysical properties of water to simulate the melting of ice spheres in water. The flow patterns around the spheres obtained by the model are compared with images from visualization studies in water performed by Hao et al. [20]. The melting times in forced convection obtained experimentally in the ice/water system by Aziz et al. [16] and Hao et al. [17] are compared with results of our numerical model. Finally, the model was compared with experimental results in aluminum and AZ91 carried out in the present work.

3.4. Melting of ice spheres in water

Aziz et al. [16] and Hao et al. [17] performed numerous investigations in the water/ice system. A series of experiments were conducted to measure forced convection heat transfer rates from submerged ice spheres in water.

The three-dimensional model was used to obtain the melting times of ice spheres under pure forced convection. The thermophysical properties of water used are shown in Table 2. The enmeshment and time step scheme used is similar to the one used for the aluminum system.

There was no mass increase observed in any of the spheres, due to the fact that their initial temperature was only −10 °C (only 10 °C below their melting point). Calculation of the Nusselt number can be seen by Eq. (8) (a particular case of Eq. (6), with $MT_F = 1$).

$$\Rightarrow Nu = \frac{\rho * LH * D_0^2}{3 * k_\infty * SPH * MT} \tag{8}$$

A series of runs were performed using a 3:6 cm ice sphere, initially at −10 °C, immersed in a water bath with superheats ranging between 10 °C and 30 °C and velocities between 0.01 m/s and 0.1 m/s. The calculated dimensionless heat transfer coefficient was obtained from Eq. (8) and was plotted along with the experimental results by Aziz et al. (Fig. 5) and Hao et al. (Fig. 6). The thin solid line in Fig. 6 represents the results obtained by Aziz et al. in 1995 and were included in the original paper by Hao et al for comparison [17]. The deviation in the Nusselt number reported on both investigations is of the order of 20%. Good agreement is observed between the numerical model and the experimental results from both experimental investigations.

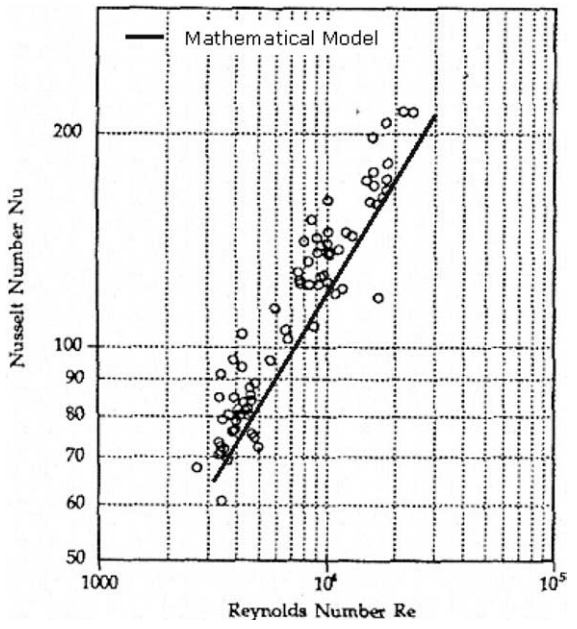

Fig. 5. Comparison between the numerical model and the experimental results by Aziz et al.

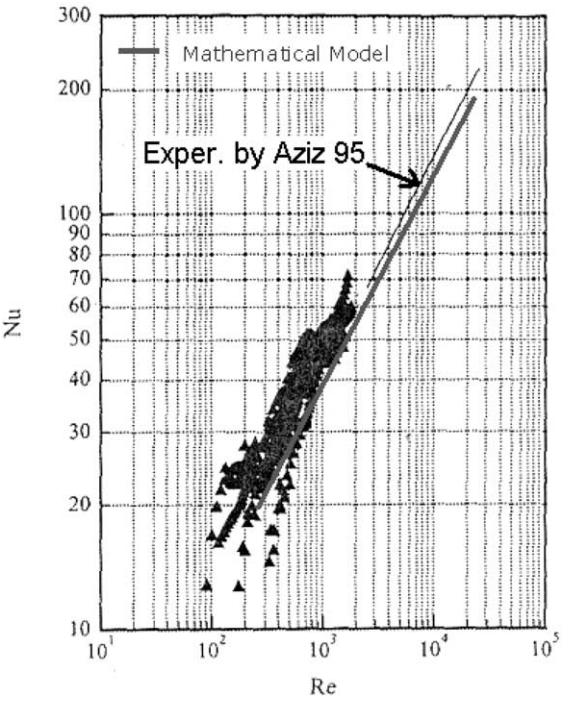

Fig. 6. Comparison between the numerical model and the experimental results by Hao et al.

4. Experimental measurements in liquid metals

4.1. Experimental work involving the revolving liquid metal tank

The apparatus used to immerse spheres consists of a cylindrical stainless steel tank that can rotate inside a heavily insulated electrical resistance furnace, called Revolving Liquid Metal Tank (RLMT). This is connected to a DC motor capable of controlling the rotating speed to a resolution of 1 RPM. The interior diameter of the RLMT is 380 mm, the height is 200 mm and it has a usable capacity of 20 l (50 kg of aluminum, approximately). Fig. 7 shows a schematic of the RLMT inside the electrical resistances furnace.

For the experiments carried out in AZ91, a protective atmosphere is used, consisting of a mixture of CO_2 and 0.5% SF_6. A stainless steel tube 1/8 in. was connected through the lid at approximately the centre of the RLMT and connected to the protective gas cylinder. The regular flow rate for the experiments was 2 l/min, although the system was calibrated to a maximum of 10 l/min of gas to be used in an emergency situation. The gas inlet can be seen in Fig. 7.

The melting time of the immersed spheres is measured by means of the change in electrical resistance between the tip of a wire inside the sphere and the bath.

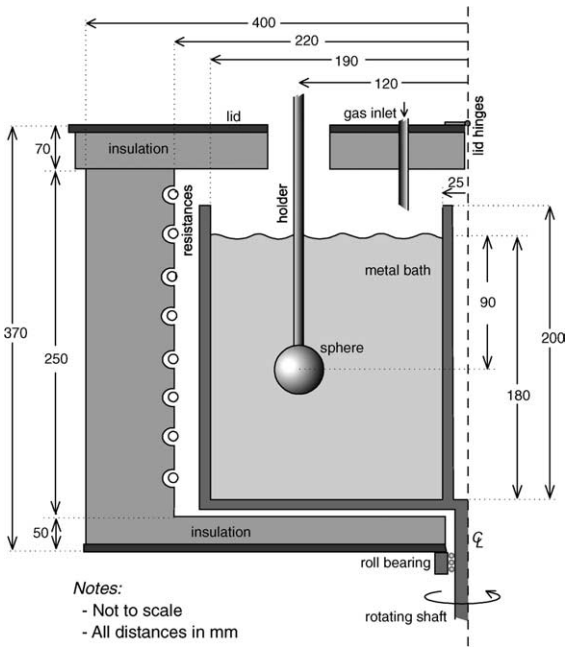

Fig. 7. Schematic of the apparatus used to immerse spheres (RLMT).

Typical results from the data acquired to measure the melting time can be found in Ref. [24].

4.2. Experimental results in liquid metals

Using the relationship between the Nusselt number and the melting time of a sphere, all the experimental results are grouped in a single graph. The results for the preheated aluminum spheres will also be included in the graph (the melting time factor used is $MT_F = 1.1$, as obtained in the numerical model). Also, the results for AZ91 will be plotted in the same graph; the melting time factor used is $MT_F = 1.5$ because AZ91 and Aluminum show very similar shell formations due to the fact that their thermophysical properties are very similar. Moreover, the Prandtl numbers of both systems are also of the same order of magnitude ($Pr_{Al} = 0.015$ and $Pr_{AZ91} = 0.024$), hence the Nusselt number expected should also be similar for the same convective condition ($Nu = f(Re, Gr, Pr)$).

All experiments carried out under forced convective conditions are grouped together in Fig. 8. This Figure includes experimental results for 3, 5 and 7 cm aluminum spheres. In these experiments, the spheres were at room temperature prior to immersion. Experimental results in which the aluminum spheres where preheated at $T_0 = 450$ °C are also shown in Fig. 8. Finally, experimental results for the AZ91 magnesium alloy are also depicted in the same figure.

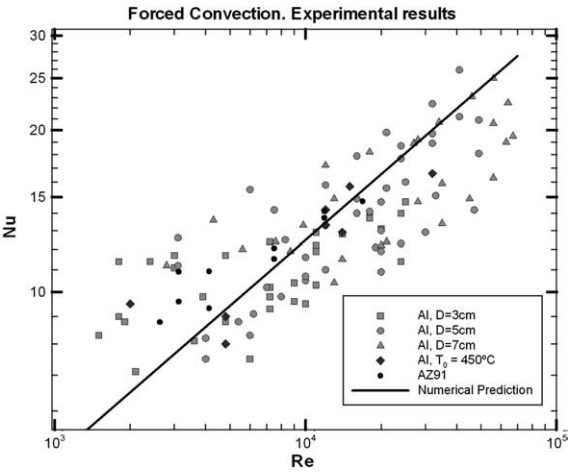

Fig. 8. Numerical model predictions and experimental results in aluminum and AZ91 in forced convection ($Pr \sim 10^{-2}$).

5. Predicting the Nusselt number for other material systems

The model has been validated with experimental results in aluminum and AZ91 ($Pr \approx 10^{-2}$) as well as with experiments in the water/ice system ($Pr \approx 10^{1}$) obtained from the literature. The Nusselt number can then be predicted for various fluids having different Prandtl numbers. This procedure was carried out by running the numerical model for several conditions corresponding to different Prandtl number fluids. With the Nusselt number obtained for values of the Reynolds and Prandtl numbers, a correlation of the form $Nu = 2 + CRe^{n_{Re}}Pr^{n_{Pr}}$ is sought. The range of values of the dimensionless parameters studied are $3 \times 10^{-3} \leqslant Pr \leqslant 10^{1}$ and $3 \times 10^{2} \leqslant Re \leqslant 3 \times 10^{4}$.

The sphere is set to be solid at the same thermal properties of the liquid and at an initial temperature equal to its melting point ($T_0 = T_m$) in order to avoid the shell formation and the subsequent error in estimating the mass increase and the melting time factor, MT_F. For each condition, the melting time is obtained and the Nusselt number is calculated using Eq. (6) with $MT_F = 1$, as done for the water/ice system.

Fig. 9 shows the Nusselt number as a function of the Prandtl number for the values of the Reynolds number studied. The slopes of the curves are almost identical among each other in the log–log plot, meaning that the exponent of the Prandtl number (n_{Pr}) is independent of the Reynolds number. Fig. 10 shows the relationship between the Nusselt and the Reynolds number for four of the eight values of the Prandtl number studied. The exponent of the Reynolds number (n_{Re}) appears to be independent of the Prandtl number.

By performing a regression analysis of the data from the results of the model, an expression for the

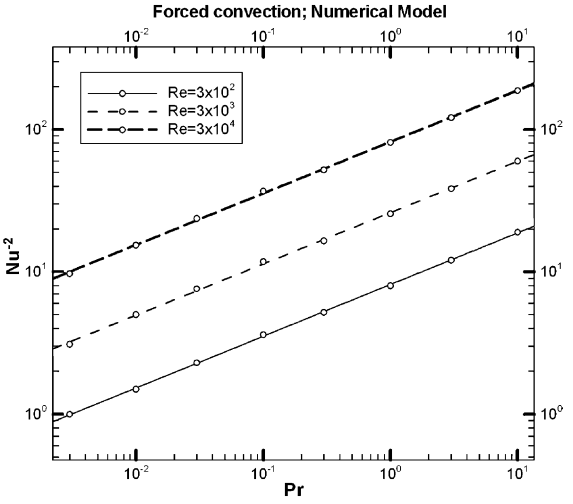

Fig. 9. Nusselt number as a function of the Prandtl number for forced convection on spheres.

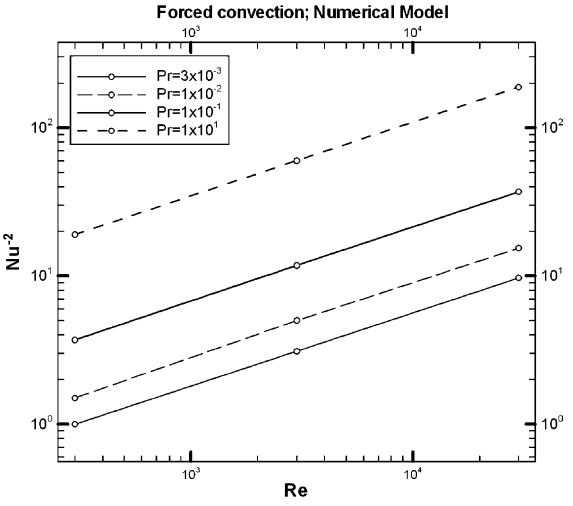

Fig. 10. Nusselt number as a function of the Reynolds number for forced convection on spheres.

dimensionless heat transfer coefficient is obtained in the range $3\times10^{-3}\leqslant Pr\leqslant10^{1}$ and $3\times10^{2}\leqslant Re\leqslant5\times10^{4}$ for the 24 points considered. The problem is as follows: find the constants $\{C, n_{Re}, n_{Pr}\}\geqslant 0$ such that I is minimized. The performance index I is given by Eq. (9). The resultant correlation is Eq. (10), with a standard deviation $\sigma_{corr}=4\%$.

$$I=\sum_{i=1}^{N}(Nu_{\mathrm{model},i}-(2+CRe_i^{n_{Re}}Pr_i^{n_{Pr}}))^2 \tag{9}$$

$$Nu=2+0.47Re^{0.5}Pr^{0.36} \tag{10}$$

Eq. (10) is used to predict the dependence of the Nusselt number on the Reynolds number for the experimental results shown in Fig. 8. In this figure, the straight solid line shows predictions based on Eq. (10). As seen, there is a good agreement between the various experimental results and predictions based on Eq. (10). The observed deviation on the lower range of Reynolds numbers is partly attributed to buoyancy effects. Uncertainty analysis on the Nusselt number estimation from Eq. (10) has shown that the error involved is of the order of 20%.

6. Conclusions

A mathematical model was developed to describe the various transport phenomena involved when a melting sphere is immersed in a moving fluid. This model was validated with various experimental results involving liquid metals and water. Based on this model, a dimensionless correlation for convective heat transfer over a sphere was developed.

$$Nu=2+0.47Re^{1/2}Pr^{0.36}\quad 3\times10^{-3}\leqslant Pr\leqslant10^{1};\quad 10^{2}\leqslant Re\leqslant5\times10^{4} \tag{11}$$

This correlation has applicability in fluids with a wide range of Prandtl numbers, and it was compared with experimental results derived in liquid aluminum and water. The comparisons have shown good agreement between predictions from the derived correlation and experimental results.

References

[1] C. Hsu, Heat transfer to liquid metals flowing past spheres and elliptical rod bundles, International Journal of Heat and Mass Transfer 8 (1965) 303–315.
[2] S. Sideman, The equivalence of the penetration theory and potential flow theories, Industrial and Engineering Chemistry Research 58 (2) (1966) 54–58.
[3] F. Kreith, L. Roberts, J. Sullivan, S. Sinha, Convection heat transfer and flow phenomena of rotating spheres, International Journal of Heat and Mass Transfer 6 (1963) 881–895.
[4] L. Witte, An experimental investigation of forced convection heat transfer from a sphere to liquid sodium, ASME Journal of Heat Transfer 90 (1968) 9–12.
[5] S. Argyropoulos, A. Mikrovas, An experimental investigation on natural and forced convection in liquid metals, International Journal of Heat and Mass Transfer 39 (1995) 547–561.
[6] S. Argyropoulos, A. Mikrovas, D.A. Doutre, Dimensionless correlations for forced convection in liquid metals: Part i. Single-phase flow, Metallurgical and Materials Transaction 32B (2001) 239–246.
[7] McAdams, Heat Transmission, third ed., McGraw-Hill, 1954.

[8] T. Yuge, Experiments on heat transfer from spheres including combined natural and forced convection, ASME Journal of Heat Transfer 82 (1960) 214–220.
[9] G. Vliet, G. Leppert, Forced convection heat transfer from an isothermal sphere to water, ASME Journal of Heat Transfer 83 (2) (1961) 163–175.
[10] C. Hieber, B. Gebhart, Mixed convection from a sphere at small reynolds and Grashof numbers, Journal of Fluid Mechanics 38 (1969) 137–159.
[11] C. Vanier, C. Tien, Free convection melting of ice spheres, AIChE Journal 16 (1970) 76–82.
[12] A. Solomon, On the melting time of a simple body with a convection boundary condition, Letters in Heat and Mass Transfer 7 (1980) 183–188.
[13] V. Eskandari, G. Jakubowski, T. Keith, Heat transfer from spherical ice in flowing water, ASME 82-HT-58.
[14] A. Anselmo, V. Prasad, J. Koziol, Melting of a sphere when dropped in a pool of melt with applications to partially-immersed silicon pellets, Heat Transfer in Metals and Containerless Processing and Manufacturing, ASME HTD 162 (1991) 75–82.
[15] A. Anselmo, V. Prasad, J. Koziol, K. Gupta, Numerical and experimental study of a solid-pellet feed continuous czochralski growth process for silicon single crystals, Journal of Crystal Growth 131 (1993) 247–264.
[16] S. Aziz, W. Janna, G. Jakubowski, A comparison of correlations for forced convection heat transfer from a submerged melting ice sphere to flowing water, ASME Heat Transfer Division 334-3 (1995) 329–334.
[17] Y. Hao, Y. Tao, Heat transfer characteristics in convective melting of a solid particle in a fluid, ASME Heat Transfer Division 364-2 (1999) 207–212.
[18] M. Mukherjee, J. Shih, V. Prasad, A visualizations study of melting of an ice sphere in a pool of water, ASME 94-WA/HT-14.
[19] P. McLeod, D. Riley, R. Sparks, Melting of a sphere in hot fluid, Journal of Fluid Mechanics 327 (1996) 393–409.
[20] Y. Hao, Y. Tao, Melting of a solid sphere under forced and mixed convection: Flow characteristics, Journal of Heat Transfer 123 (5) (2001) 937–950.
[21] R. Nordlie, F. Kreith, Convection heat transfer from a rotating sphere, International Developments in Heat Transfer, ASME (1961) 461–467.
[22] E. Sparrow, R. Eichhorn, J. Gregg, Combined forced and free convection in a dary layer, Physics of Fluids 2 (3) (1959) 319–328.
[23] B. Melissari, S. Argyropoulos, The identification of transition convective regimes in liquid metals using a computational approach, Progress in Computational Fluid Dynamics, an International Journal 4 (2) (2004) 69–77.
[24] B. Melissari, S. Argyropoulos, Measurement of magnitude and direction of velocity in high temperature liquid metals. Part I: Mathematical modeling and Part II: Experimental measurements, Metallurgical and Materials Transactions, (2005), in press.
[25] S. Paterson, Propagation of a boundary of fusion, Proceedings Glasgow Mathematical Association 1 (1952) 42–47.
[26] B. Melissari, The sphere melting technique: mathematical modelling, Experimental Measurements and Applications, Ph.D. Thesis, University of Toronto, 2004.
[27] C. Gau, R. Viskanta, Melting and solidification of a pure metal on a vertical wall, ASME Journal of Heat Transfer 108 (1986) 174–181.
[28] S. Whitaker, Forced convection correlations, AIChE Journal 18 (2) (1972) 361–371.
[29] E. Turkdogan, Physical Chemistry of High Temperature Technology, Academic Press, 1980.